Research Square

Preprints are preliminary reports that have not undergone peer review.
They should not be considered conclusive, used to inform clinical practice,
or referenced by the media as validated information.

Flexible and Attachable Terahertz Polarizer Enabled by Laser-induced Graphene

Jia Zhang
Beijing Institute of Technology
Keke Wang
Beijing Institute of Technology
Xudong Wu
Beijing Institute of Technology
Haoyang Li
Beijing Institute of Technology
Juan Liu
Beijing Institute of Technology
Bin Hu
hubin@bit.edu.cn
Beijing Institute of Technology

Research Article

Keywords: terahertz, laser-induced graphene, polarizer, direct laser writing, flexible device

Posted Date: November 9th, 2026

DOI: https://doi.org/10.21203/rs.3.rs-11396365/v1

License: This work is licensed under a Creative Commons Attribution 4.0 International License.
Read Full License

Additional Declarations: No competing interests reported.

Flexible and Attachable Terahertz Polarizer Enabled by Laser-induced Graphene

Jia Zhang[a,b,c], Keke Wang[a,b], Xudong Wu[a,b], Haoyang Li[a,b], Juan Liu[a,b] and Bin Hu[a,b,*]

[a] *School of Optics and Photonics, Beijing Institute of Technology, Beijing, 100081, China*

[b] *National Key Laboratory on Near-Surface Detection, Beijing, 100072, China*

[c] *China Academy of Aerospace System and Innovation, Beijing 100088, China*

These authors contributed equally: Jia Zhang, Keke Wang.

E-mail: *hubin@bit.edu.cn*

Abstract

Terahertz (THz) polarizers are indispensable for polarization-sensitive spectroscopy, imaging, and communication systems. Conventional metal-based wire-grid polarizers, despite their high performance, rely on complex photolithography and thin-film deposition processes that incur substantial costs and constrain scalability. Here, we demonstrate a flexible and attachable THz polarizer enabled by laser-induced graphene (LIG)—a three-dimensional porous carbon material synthesized in a single step via direct laser writing on polyimide. The polarizer consists of 2 layers of LIG wire-grid geometry with a period of 60 μm and a strip width of 50 μm, and is fabricated through a streamlined, mask-free protocol and subsequently peeled from its rigid substrate for transfer onto arbitrary flexible supports. Experimental results show that the polarizer yields an extinction ratio less than −25 dB across 0.25–1.0 THz, and this value keeps no more than -20 dB under bending radii down to 22.5 mm. These results establish LIG as a compelling material platform for low-cost, scalable, and transferable THz polarizers, bridging the gap between high-performance metal-based devices and practical manufacturing requirements.

Keywords: terahertz; laser-induced graphene; polarizer; direct laser writing; flexible device

1. Introduction

Terahertz (THz) waves occupy a unique position in the electromagnetic spectrum between microwaves and infrared light, exhibiting both electronic and photonic characteristics [1,2]. In recent years, THz technology has attracted widespread attention due to its promising applications in high-speed wireless communications [3,4], security screening [5], biomedical imaging [6], and non-destructive material inspection [7]. The low photon energy of THz radiation ensures minimal ionization damage to biological tissues, making it particularly attractive for medical diagnostics [8]. Additionally, the "fingerprint" spectral features of numerous molecules in the THz range enable substance identification and hazardous material detection [9,10].

In all these applications, polarization modulation plays a vital role from enlarging information capacity to improving detection precision and diversifying inspection approaches [11]. As a basic and key polarization modulator, traditional THz polarizers are composed of wire-grid structures, which have high transmission and extinction ratio (ER) [12,13]. By multi-layer stacked structures, the ER is able to reach as high as 90 dB [14]. By fabricating the wire-grid polarizer (WGP) on a flexible substrate, the polarizer can be even bent with a small radius of curvature (ROC), providing the device with a wider range of application prospects [15,16]. However, the fabrication of this structure relies on photolithography technique, which is high cost. More importantly, poor ductility of the wire-grid material may lead to structural delamination under bending deformation. To solve these problems, carbon nanotubes were selected [17,18]. Nevertheless, further attempts are still required.

Laser-induced graphene (LIG), first reported by Lin et al. in 2014 [19], represents a paradigm shift in graphene synthesis. By irradiating commercial polyimide (PI) films with a CO_2 infrared laser, three-dimensional porous graphene structures are generated in a single step, without the need for high-temperature furnaces, chemical vapor deposition systems, or post-growth transfer processes. The resulting LIG exhibits high electrical conductivity (5–25 $S \cdot cm^{-1}$) and excellent thermal stability (>900 °C). Crucially, the laser direct-writing process enables arbitrary patterning of LIG with micrometer-scale resolution, opening new avenues for rapid, low-cost, and mask-free fabrication of

graphene-based electronic and photonic devices [20]. Recent studies have revealed that LIG exhibits metallic behavior in the THz regime, characterized by low transmittance and high reflectance [21]. LIG-based metasurfaces can be designed to have functions like focusing and holography [22]. These findings establish the feasibility of LIG as a functional material for THz devices.

In this work, through parameter optimization, we design a two-layered THz WGP consisting of LIG, PI, and polyurethane (PU). Due to the advantages of laser-direct writing, the device is low-cost, fast fabricated, and has high alignment accuracy. Besides the function of flexibility, it can also be peeled off from the substrate and attached to another flexible substrate. Our results position LIG as a compelling material platform for low-cost, scalable, and patternable THz polarizers, complementing existing metal-based and transparent-conductive-oxide-based approaches.

2. Design Principle and Simulation

The operating principle of a WGP relies on the anisotropic interaction between the incident electromagnetic wave and conductive strips. For the electric field component perpendicular to the grating direction (parallel to the grid lines), as shown in Fig. 1(a), free electrons in the conductor oscillate along the strip direction, re-radiating energy in both forward and backward directions. The forward re-radiation destructively interferes with the incident wave, while the backward component constitutes reflection. Conversely, for the electric field component parallel to the grating direction, electron motion across the narrow gaps between strips is inhibited. Instead, the incident wave excites surface plasmon polaritons at the gaps, thereby enabling extraordinary optical transmission for the parallel polarization. The effectiveness of this mechanism requires the grid period to be smaller than the operating wavelength.

In this work, LIG is employed as the conductive material in a WGP because its metallic character in the THz band has been confirmed [21]. The finite-difference time-domain (FDTD) method is employed to optimize the parameter of a single layer LIG polarizer. The schematic of the structure is depicted in Fig. 1(a). The WGP lies in the *x*–*y*

plane, with a period of p. The width of a LIG strip is denoted by a. The thickness of the PI substrate is 80 μm.

Because LIG exhibits electrical conductivity that depends strongly on the laser energy density, we first decide the polarization performance under different fabrication energy density. The permittivity of LIG is obtained by experimentally measured data in our previous work [22]. The simulation results are shown in Fig. 1(b). In the 0.1–1.0 THz band, the parallel polarization exhibits an average transmission of approximately 50% for all fabrication energy densities, whereas the transmission for the vertical polarization remains low and decreases with the laser energy density. At 0.6 THz, the transmission is on the order of 10^{-3} for an energy density of 68 J·cm^{-2}, and on the order of 10^{-6} for 132.6 J·cm^{-2}. This is because LIG conductivity increases monotonically with laser energy density [22]. Therefore, the LIG permittivity corresponding to 132.6 J·cm^{-2} is adopted for the subsequent design.

We then optimize the period and strip width, and the results are shown in Fig. 1(c) and (d), respectively. As the period decreases from p = 200 μm to p = 60 μm at a fixed duty cycle of 0.5, the parallel transmission remains almost unchanged, whereas the vertical transmission decreases. At 0.8 THz, the transmission drops from 10^{-2} to 10^{-6}. When the period is fixed at p = 60 μm, both parallel and vertical polarization transmissions decrease with the strip width. But the decline in vertical polarization transmission exceeds that of parallel polarization, indicating that a higher extinction ratio is achieved for larger strip widths.

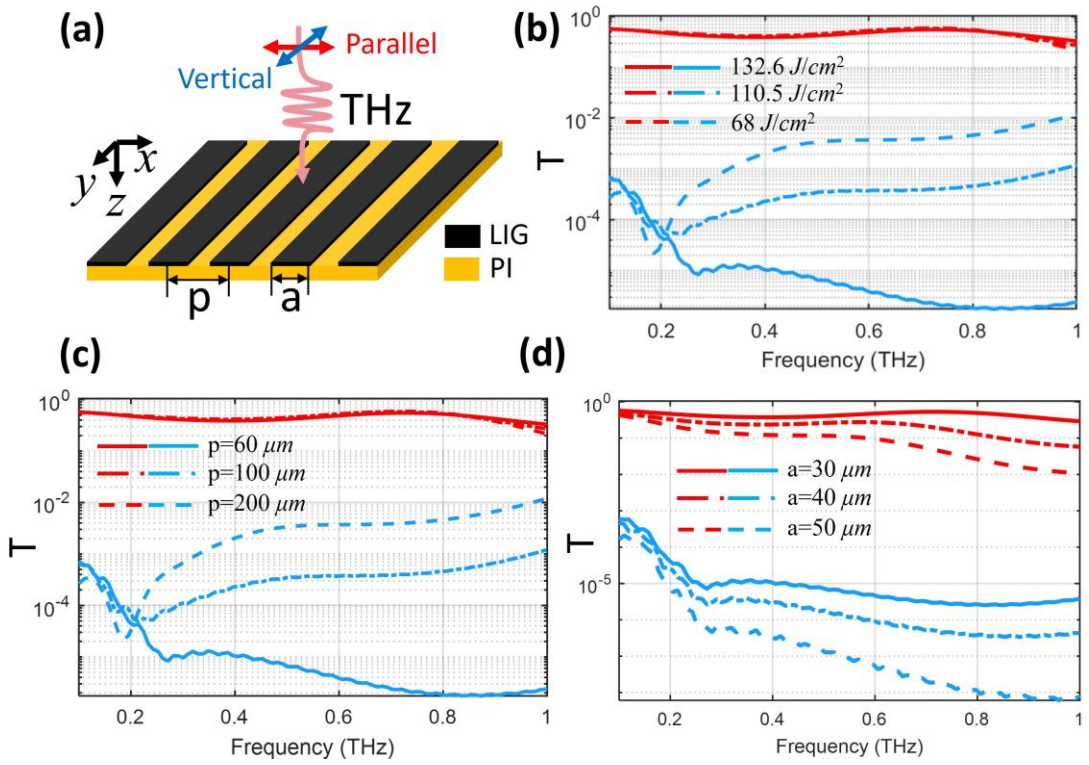


Figure 1. LIG polarizer and its parameter optimization. (a) Schematic of a single layer LIG WGP. (b) Simulated transmission of the parallel and vertical polarizations under different laser-inducing power. (p=60μm, a=30μm) (c) Simulated transmission of the parallel and vertical polarizations under different periods (a=p/2). (d) Simulated transmission of the parallel and vertical polarizations under different LIG width (p=60μm).

The ER of the single layer LIG polarizer is depicted as the blue line in Fig. 2, which is defined as:

$$ER = 10\log_{10}\left(\frac{T_{\perp}}{T_{\parallel}}\right)$$

in which $T_{\perp}$ is the transmission of vertical polarization, and $T_{\parallel}$ is the transmission of parallel polarization. It can be seen from the simulation results that the ER is -32 dB at 0.1 THz. It decreases with the frequency and reaches its minimum value of -60 dB at 0.7 THz, which is comparable to other THz WGP designs [13,15,17].

In order to increase the ER of the LIG polarizer, we adopt a mismatched double layer (MDL) structure similar to Ref. [14], which consists of two LIG wire-grid layers with the identical geometric structures but displaced by half period, as shown by the inset of Fig. 2. To facilitate subsequent fabrication, the two LIG wire-grid layers are separated by an 80-μm polyimide substrate. The simulated ER is shown as the red curve in Fig. 2, which clearly demonstrates that the MDL structure suppresses the ER. For frequencies above 0.2 THz, the ER falls below −100 dB, indicating excellent polarizer performance. Taking all the above results into account, geometric parameters of p = 60 μm and a = 50 μm are selected for fabrication.

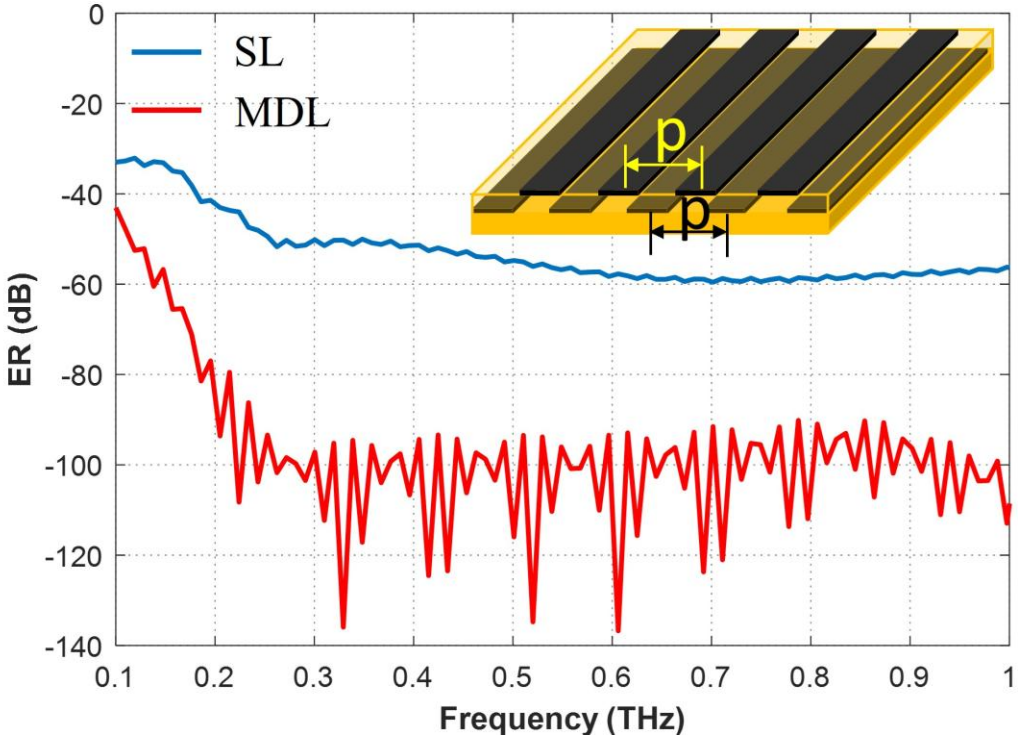


Figure 2. Simulated extinction ratio (ER) of a single layer (SL) LIG WGP and a mismatched double layer (MDL) LIG WGP. (p=60μm, a=50μm)

3. Fabrication

The LIG polarizers are fabricated using a custom-built laser direct-writing system [22]. The system employs a Nd:YVO_4 nanosecond solid-state laser (532 nm wavelength, 15 ns pulse width, adjustable repetition rate) equipped with a beam expander and a 60-

mm focal-length scanning lens. A dual-mirror galvanometer scanning system steers the focused laser beam in the *x* and *y* directions, enabling patterning over an 18 mm × 18 mm working area. The laser scanning speed is fixed at 50 mm/s.

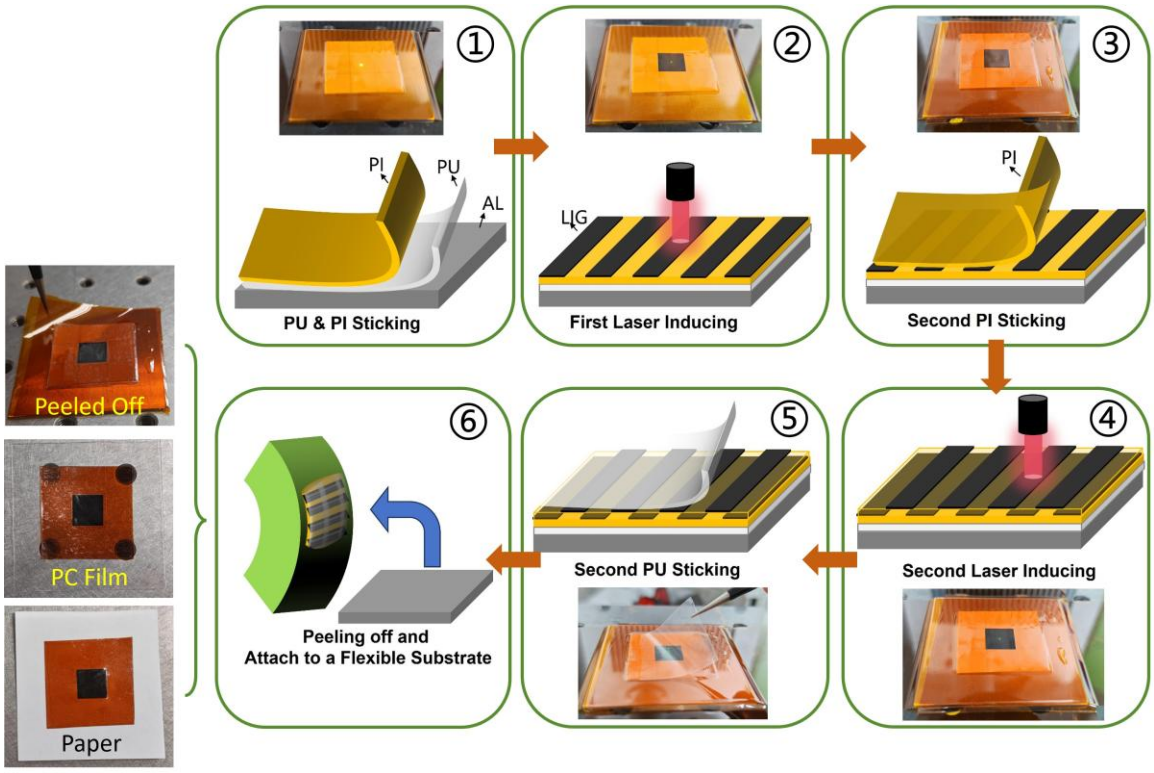


Figure 3. Fabrication process. The photos on the right, from top to bottom: peeled off LIG polarizer, the LIG polarizer attached to a PC film, the LIG polarizer attached to a paper.

Multilayer LIG metamaterials have been demonstrated to be fabricated using repeatedly laminating PI and PU films followed by laser direct writing [23]. Using this technique, the MDL LIG polarizer is fabricated through a streamlined, mask-free protocol, as depicted in Fig. 3. First, a PU layer (80 μm) and a PI tape are sequentially adhered to an aluminium substrate, followed by laser ablation to convert the PI into LIG wire-grids for the first layer. A second PI tape is then adhered to the first layer, followed by laser-induced conversion of the second LIG wire-grid pattern. In the fifth step, another PU tape is adhered to the second LIG layer as a protective cover to prevent LIG detachment. Finally, because the adhesion between the first PU layer and the Al substrate

is relatively weak, the entire MDL LIG polarizer can be carefully peeled off and transferred to another flexible substrate. We transfer the LIG polarizers to a polycarbonate (PC) film and a sheet of paper, respectively, as shown on the left of Fig. 3.

Photograph of the peeled off LIG polarizer, its microstructure under an optical microscopy, and its morphological features examined by scanning electron microscopy (SEM) are shown in Fig. 4. Microscopic examination confirms that the fabricated geometric structure aligns with the design. The fabricated wire-grid width is approximately a = 50.77 μm. SEM imaging also reveals the porous structure of LIG, with pore sizes below 10 μm, which is a characteristic feature of LIG.

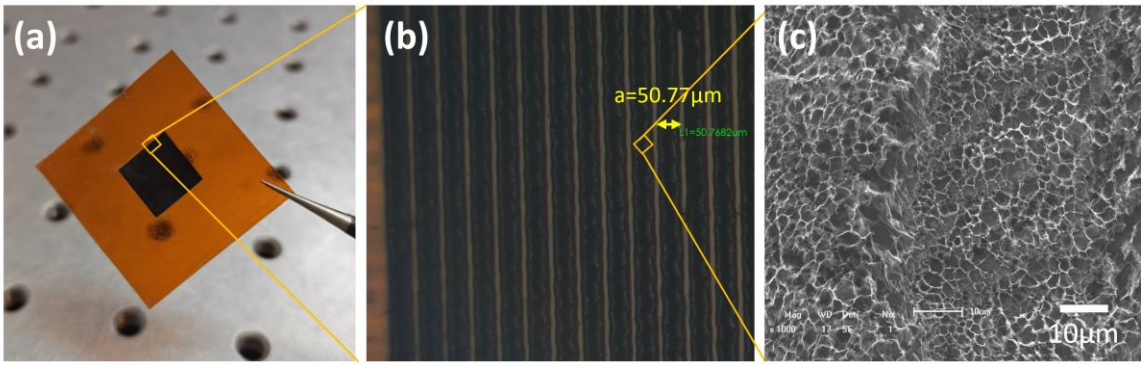


Figure 4. Fabricated LIG polarizer. (a) Photos of the LIG polarizer. (b) Microscope image. (c) SEM image.

4. Experimental Results and Discussion

The THz transmission properties of the fabricated polarizers are measured using a THz time-domain spectroscopy (THz-TDS) system [23]. The measured transmission and corresponding ER for the polarizers on PC and paper substrates are shown in Fig. 5. Fig. 5(a) shows that for both parallel and vertical polarizations, the transmission through the PC substrate is lower than that through the paper substrate, because paper is highly transparent to THz waves. It is also found that the measured transmission of the MDL LIG polarizer is of the same order as the simulated transmission of the SL LIG polarizer. This result is also found in the ER spectrum shown in Fig. 5(b). For both PC and paper substrates, the ER ranges from −15 to −50 dB, which is of the same order as that of the SL structure shown in Fig. 2. The discrepancy between the experimentally measured ER

of the MDL structure and the simulation results is attributed to fabrication errors and substrate absorption.

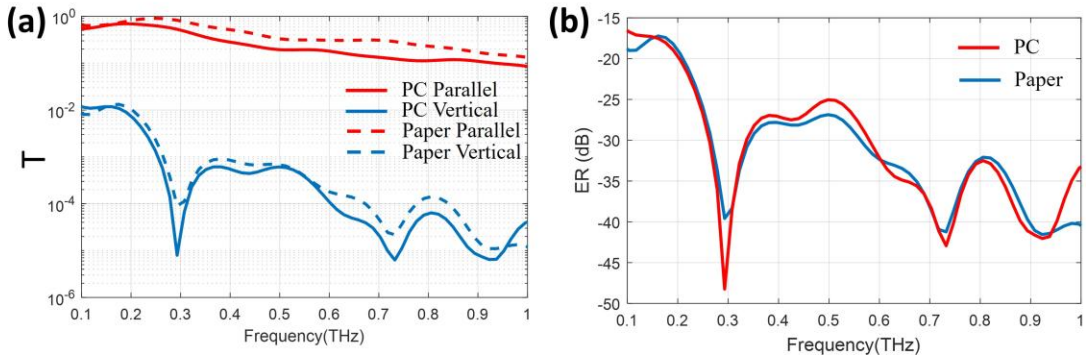


Figure 5. Experimental results of (a) transmission and (b) extinction ratio of the LIG polarizer with PC and paper substrates.

We then measured the flexible performance of the device under different radius of curvatures (ROCs). For transmission measurements, LIG polarizers are fixed on a 3D printed holder, equipped with various slots to achieve different ROCs, as shown in Fig. 6(a). The experimental ER spectra for the PC and paper substrates are shown in Fig. 6(b) and (c), respectively. For both substrates, the ER decreases with the degree of bending. For example, at 0.3 THz, the ER increases from −49 dB to −26 dB for the PC substrate, and from −40 dB to −18 dB for the paper substrate. This is attributed to the increased air gap between the two LIG wire-grid layers upon bending, which permits greater transmission of the vertical polarization component.

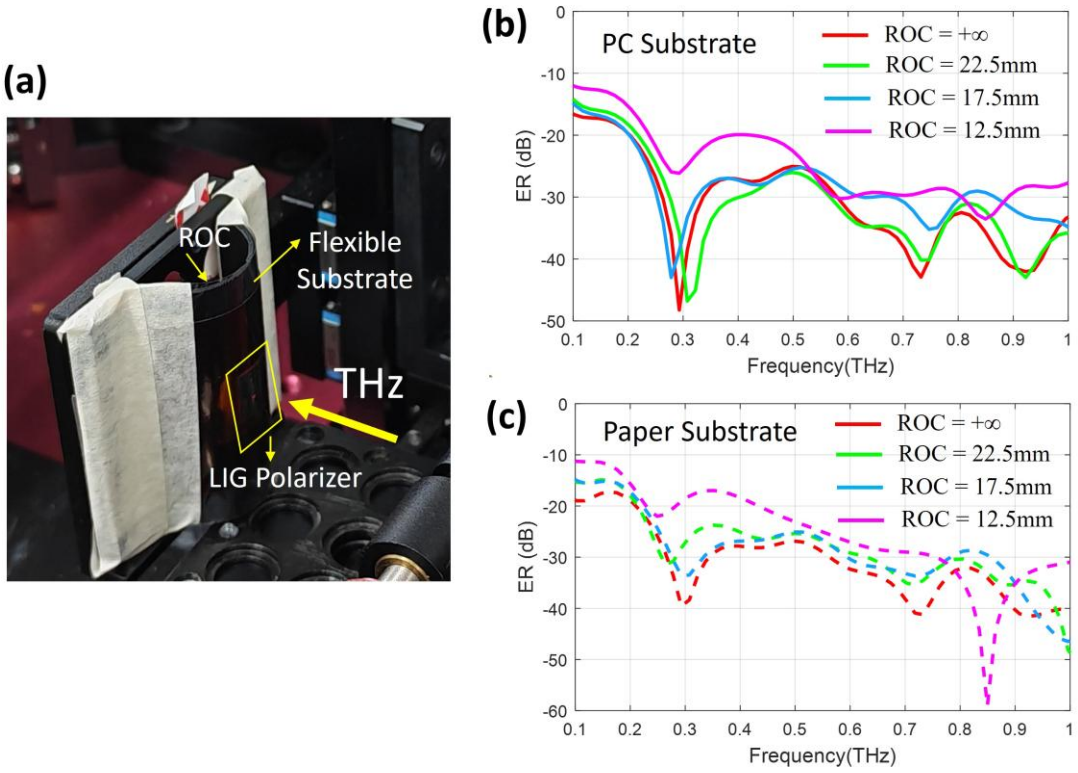


Figure 6. Experimental results of flexibility performance. (a) Photo of the bent LIG polarizer with a PC substrate. ROC indicates the radius of curvature. (b) Extinction ratio of the LIG polarizer on a PC substrate under different ROC. (c) Extinction ratio of the LIG polarizer on a paper substrate under different ROC.

Table 1 presents a comparison of our LIG polarizers with representative THz polarizers from the literatures, including metal-based metamaterial polarizers [14], transparent-conductive-oxide devices [16], and carbon nanotube polarizers [18]. Several conclusions can be drawn from this comparison. Metal-based metamaterial polarizers achieve the highest extinction ratios and broadest bandwidths, but their fabrication requires complex, multi-step MEMS processing in a cleanroom environment. ITO-based flexible polarizers offer optical transparency in the visible range and good flexibility, but they still rely on photolithography. Our LIG polarizers occupy a unique niche: they deliver moderate yet competitive ER performance through an exceptionally simple, mask-free fabrication process that is inherently scalable and compatible with arbitrary patterning.

Table 1. Polarizer comparison

Parameter	Park et al. [14]	Lai et al. [16]	Zubair et al. [18]	This Work
Material	Au	ITO	Carbon nanotube	LIG
Fabrication	MEMS photolithography	Sputtering + photolithography	Manually winding	Laser direct-write
Substrate	PI (3 μm)	PET (129 μm)	Free-standing	PI (80 μm)
Period	7 μm	20 μm	20 μm in average	60 μm
ER	−90 dB	-24 dB	−30 dB	−48 dB
Bandwidth(<−25 dB)	0.2–2.5 THz	0.1–2.5 THz	0.2–1.1 THz	0.25–1.0 THz
Cost	High	Medium	Low	Low
Scalability	Low (cleanroom)	Medium	Low	High (mask-free)
Flexibility	Yes (thin PI)	Yes (PET)	Not mentioned	Yes
Transferability	No	No	No	Yes

5. Conclusion

In summary, we have demonstrated a flexible and attachable terahertz polarizer based on LIG, encompassing electromagnetic design, mask-free fabrication, and experimental validation. FDTD simulations confirm that LIG exhibits metallic behaviour in the 0.1–1.0 THz range, and a parametric study identifies a wire-grid period of 60 μm and strip width of 50 μm as an optimal compromise between extinction performance and fabrication resolution. The adoption of a mismatched double-layer architecture—in which two identical LIG gratings are offset by half a period—dramatically suppresses transmission of the unwanted polarization, yielding a simulated extinction ratio below −100 dB for frequencies above 0.2 THz. Experimentally, the polarizer is fabricated through a one-step, mask-free laser direct-writing process and subsequently peeled from its rigid substrate for transfer onto arbitrary flexible supports, including PC film and paper. THZ-TDS yields a measured extinction ratio of −48 dB across 0.25–1.0 THz, with robust polarizing capability retained under bending radii as small as 22.5 mm. These results establish LIG as a viable, low-cost, and scalable material platform for THz polarizers.

Declarations

Ethical Approval
Not applicable. This study involves neither human participants nor animal subjects.

Funding
This work was supported by the Beijing Natural Science Foundation (F251051) and the Beijing Natural Science Foundation (No. L223031).

Availability of data and materials
The datasets generated and analysed during the current study are available from the corresponding author on reasonable request.

Competing Interests
The authors declare no competing financial or personal interests.

References

[1] Nagatsuma T, Ducournau G and Renaud C 2016 *Nature Photonics* **10** 371

[2] Tonouchi M 2007 *Nature Photonics* **1** 97

[3] Akyildiz I F, Jornet J M and Han C 2014 *Physical Communication* **12** 16

[4] Federici J F, Schulkin B, Huang F, Barat R, Oliveira F and Gary D 2005 *Semiconductor Science and Technology* **20** S266

[5] Kawase K, Ogawa Y, Watanabe Y and Inoue H 2003 *Optics Express* **11** 2549

[6] Pickwell E and Wallace V P 2006 *Journal of Physics D: Applied Physics* **39** R301

[7] Yang X, Wu T, Zhang L, Yang D, Wang N N, Song B and Gao X B 2019 *Signal Processing* **160** 202

[8] Yu C, Fan S, Sun Y and Pickwell-MacPherson E 2012 *Quantitative Imaging in Medicine and Surgery* **2** 33

[9] Ho L, Pepper M and Taday P 2008 *Nature Photonics* **2** 541

[10] Laman N, Harsha S S, Grischkowsky D and Melinger J S 2008 *Biophysical Journal* **94** 1010

[11] Huang S-X, Wu G-B, Chan K-F, Chen B-J, Xia M-Y, Fromenteze T, Decroze C and Chan C H 2021 *Optics Express* **29** 14853

[12] Yamada I, Takano K, Hangyo M, Saito M and Watanabe W 2009 *Optics Letters* **34** 274

[13] Takano K, Yokoyama H, Ichii A, Morimoto I and Hangyo M 2011 *Optics Letters* **36** 2665

[14] Park H, Park H, Lee J, Shim J, Son H, Park J, Baek S and Kim T-T 2024 *APL Photonics* **9** 110807

[15] Ferraro A, Zografopoulos D C, Missori M, Peccianti M, Caputo R and Beccherelli R 2016 *Optics Letters* **41** 2009

[16] Lai W, Yuan H, Fang H, Zhu Y and Wu H 2020 *Journal of Physics D: Applied Physics* **53** 125109

[17] Ren L, Pint C L, Arikawa T, Takeya K, Kawayama I, Tonouchi M, Hauge R H and Kono J 2012 *Nano Letters* **12** 787

[18] Zubair A, Tsentalovich D E, Young C C, Heimbeck M S, Everitt H O, Pasquali M and Kono J 2016 *Applied Physics Letters* **108** 141107

[19] Lin J, Peng Z, Liu Y, Ruiz-Zepeda F, Ye R, Samuel E L G, Yacaman M J, Yakobson B I and Tour J M 2014 *Nature Communications* **5** 5714

[20] Chyan Y, Ye R, Li Y, Singh S P, Arnusch C J and Tour J M 2018 *ACS Nano* 12 2176

[21] Wang Z, Wang G, Liu W, Hu B, Wu X, Zeng Z, Li H and Zhang M 2020 *Journal of the Optical Society of America B* **37** 546

[22] Wang Z, Wang G, Hu B, Liu W, Zeng Z, Li H, Zhang M and Rosker M 2022 *Carbon* **187** 256

[23] Wu X, Xiong C, Li H, Liu W, Tao J and Hu B 2026 *Carbon* **254** 121520